*Research Article*

# Synthesis of Composite Hydrogel Made of Woven Fabrics Stitched with PVA Yarn

**Faheem Ahmad** [iD],[1] **Farooq Azam** [iD],[1] **Faaz Ahmed Butt** [iD],[2] **Abher Rasheed** [iD],[1] **Yasir Nawab** [iD],[1] **and Sheraz Ahmad** [iD][1]

[1]*School of Engineering & Technology, National Textile University, Faisalabad 37610, Pakistan*
[2]*Materials Engineering Department, NED University of Engineering and Technology, Karachi, Pakistan*

Correspondence should be addressed to Sheraz Ahmad; sheraz@ntu.edu.pk

In this study, a new method to prepare polyvinyl alcohol (PVA) hydrogel-based woven fabric composite is presented. In this method, the woven fabric was first stitched with PVA yarn and then subjected to the borax solution for simultaneously dissolving and crosslinking PVA. The prepared PVA hydrogel-based woven fabric composite was chemically, mechanically, and thermally characterized. FTIR analysis was performed to confirm the crosslinking of PVA on the reinforced fabric surface. X-ray diffraction analysis was carried out to investigate the crystallinity of the composite. An optical microscope was used to investigate the surface morphology of the composites. Moreover, a DSC analysis was done to investigate the thermal characteristics of the composite. The mechanical and fluid absorbency characteristics of the composite were analyzed to investigate the effect of the concentration of PVA yarn on the tensile strength and water absorbency of composites. The results showed that the tensile strength and rigidity of the composite increased by increasing the PVA yarn content in the composite.

## 1. Introduction

Hydrogels are considered a class of polymeric materials that have high porosity, flexibility, and water retention capacity which make them attractive for biomedical applications such as tissue engineering, wound dressings, cell culture, sanitation products, and drug delivery materials [1, 2]. Hydrogels are usually prepared from a 3D network of hydrophilic natural or synthetic polymers through several chemical methods [3]. These chemical methods include the formation of hydrogels by single-step polymerization or multistep process containing the synthesis of polymers with several reactive groups and later their crosslinking by using various crosslinking agents. The crosslinked structure of hydrogels enables them to absorb and retain a huge amount of water without dissolving in it [4, 5]. The hydrogels for biomedical applications are synthesized by employing water-soluble polymers which include polysaccharides, polyvinylpyrrolidone, polyacrylic acid, polyacrylamide, and

polyvinyl alcohol. Polyvinyl alcohol (PVA) has the huge advantage of being biocompatible, nontoxic, and easy to synthesize into a hydrogel. Therefore, it is extensively used and studied in the literature for various medical applications [6, 7].

Polyvinyl alcohol (PVA) hydrogels are commonly employed as drug carriers in various drug delivery systems. PVA-based drug delivery systems have demonstrated superior performance in terms of extending drug release, and the release time can be easily regulated and controlled. Additionally, these drug delivery systems have shown promising results in treating cancer and diabetes patients [8, 9]. The PVA hydrogel wound dressings are found to be well permeable to air and keep the wound moist which helps to heal the wound quickly [10, 11]. PVA hydrogels are also used as an alternative to the articular cartilage [12, 13]. Moreover, PVA hydrogels are also utilized as temperature sensors and conductive and antifreeze materials [14, 15]. Even though PVA hydrogels have several applications, their

low mechanical properties such as breaking and tear strength are the major issues.

The fibers which are manufactured from PVA are suitable to blend with natural fibers such as cotton, flax, and wool. This blend is used to form an eco-friendly composite material. This interaction contributes to PVA-natural fiber composites having unique properties and good mechanical performance. It also shows a good interaction between reinforcement and matrix materials [16]. Generally, the mechanical strength of natural fibers such as cotton and flax obtained from plant sources is mostly influenced by so many factors such as moisture content, amount of cellulose, microfibrillar angle, temperature, and amount of defect present on the fibers [17–19]. The mechanical performance of the cotton and flax fibers is enhanced when the fibers are exposed to wet condition and lose their strength in dry moisture content while the mechanical strength of wool fibers is decreased in wet condition and increased in dry conditions [20].

Various strategies are adopted to enhance the mechanical properties of PVA hydrogels [21–23]. One of the strategies is to prepare PVA hydrogel-based composites by using textile materials such as fibers/filaments, yarns, and fabrics as reinforcements [24]. These PVA hydrogel-based composites are usually manufactured by preparing a PVA solution and then soaking the reinforcement (which is normally a woven fabric) in the PVA solution. Afterward, the PVA is crosslinked on the soaked fabric by using a suitable chemical agent such as boric acid and aldehydes to produce a fabric-reinforced PVA hydrogel structure. The used reinforcements (fabrics) are prepared with common fibers/yarns such as polyester, polypropylene, and glass [25–27]. This strategy is also common to prepare other types of hydrogel fabric-reinforced composites such as alginate and cellulose-based hydrogel composites [28, 29].

Recently, studies reported another strategy to prepare a PVA hydrogel-based composite by inserting PVA yarn/fibers in the weft direction of the fabric which was later crosslinked by borax. According to the literature, the mechanical properties of PVA hydrogel composites are better than those of pure PVA hydrogels. However, this process is time-consuming since the fabric must be woven first and then transformed into a hydrogel composite. Additionally, it does not allow for the use of any preexisting fabric to be converted into a hydrogel composite [30].

The present study proposes a new method to address the aforementioned issue of preparing PVA hydrogel-based composites. In this method, the PVA yarn was stitched on any desired woven fabrics and the crosslinking of PVA was done by using borax to achieve a PVA hydrogel woven fabric composite. Three different kinds (flax, jute, and polypropylene) of fabric were selected as reinforcements to produce a PVA hydrogel woven fabric composite. This method gives the freedom to choose any already prepared fabric and stitch the PVA yarn on it in the required quantity and convert it into hydrogel composite rather than putting the PVA yarn into weft during the manufacturing process of fabric. The prepared PVA hydrogel woven fabric composites by this method have good mechanical properties and have

great potential to be used in various PVA hydrogel-based applications.

## 2. Materials and Method

PVA yarn having linear density (30/1) was purchased from Coats Ltd. Borax ($Na_2B_4O_7$, MW = 201.2) was purchased from DAEJUNG, Korea. All materials are used as received. Flax, polypropylene, and jute woven fabrics were obtained from National Textile University Faisalabad, Pakistan. The design of experiment for this study is given in Table 1.

*2.1. Method.* All the fabrics (flax, polypropylene, and Jute) were first stitched with PVA yarn using different fiber volume ratios (0.20%, 0.25%, and 0.30% o.w.f). Then, a 1 wt % solution of borax in water was prepared separately using magnetic stirring at 50°C. Afterward, the stitched fabric was taken into a Petri dish and the borax solution was poured onto it so that the fabric got dipped in the solution to transform the PVA yarn into hydrogel using crosslinking of PVA molecules in the fabric structure. The schematic diagram to prepare the PVA hydrogel woven fabric composite is shown in Figure 1.

Since PVA was in the fibrous form which has a high surface area, there was no need to heat the solution for the dissolution of PVA. PVA got dissolved just after getting in contact with water. So, with the presence of the crosslinking agent (borax) in the water, PVA yarn simultaneously dissolved and crosslinked to convert the stitched fabric into the hydrogel structure. After that, the sample was kept in solution for 24 hours for proper gelation. After 24 hours, the excess borax/water solution was removed, and the hydrogel sample was washed with distilled water so that uncrosslinked molecules can be removed. After washing, samples were dried at room temperature.

### 2.2. Characterization

*2.2.1. Surface Morphology.* The fibers' surface morphology was examined with scanning electron microscopy (SEM) and optical microscopy with 180X magnification by a Labomed CZM6 stereo microscope. However, since the samples were nonconductive, they were coated with gold using a sputter coater before SEM analysis.

*2.2.2. FTIR Analysis.* Fourier-transform infrared spectroscopy analysis was carried out by using a PerkinElmer FTIR spectrometer between the ranges of 650 and 4000 cm$^{-1}$. FTIR spectroscopy is performed on the fabrics before and after gelation to carry out the chemical analysis.

*2.2.3. Differential Scanning Calorimetry (DSC) Analysis.* A differential scanning calorimeter (DSC 400, PerkinElmer) was used for the investigation of the thermal properties of the hydrogel composite. The rate of heating/cooling was set to 5°C/min.

TABLE 1: Design of experiment.

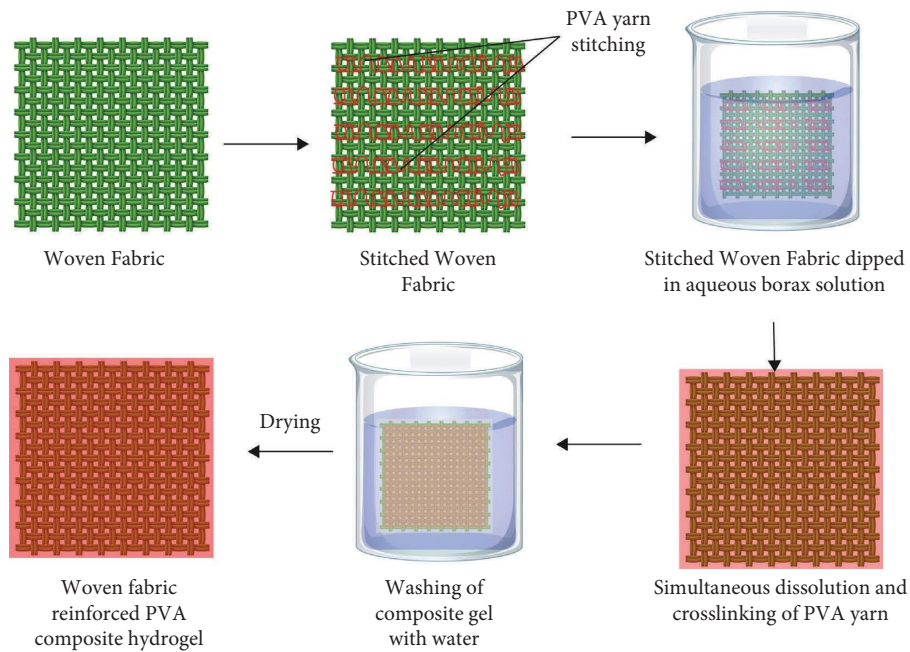| Sample ID | PVA yarn fraction (o.w.f) | Woven fabric type |
| --- | --- | --- |
| 1 | 0.20 | Flax fabric |
| 2 | 0.25 | Flax fabric |
| 3 | 0.30 | Flax fabric |
| 4 | 0.20 | Polypropylene fabric |
| 5 | 0.25 | Polypropylene fabric |
| 6 | 0.30 | Polypropylene fabric |
| 7 | 0.20 | Jute fabric |
| 8 | 0.25 | Jute fabric |
| 9 | 0.30 | Jute fabric |



FIGURE 1: Process flow to prepare PVA hydrogel woven fabric composite.

*2.2.4. X-Ray Diffraction Analysis.* Microstructural information on hydrogel composites was obtained by using the X-ray diffraction (X'Pert Pro, PANalytical) technique. To investigate the composite samples, the copper anode was employed as an X-ray source which was supplied with a current of 30 mA at 40 kV to produce a wavelength of 0.1540 nm. The data were obtained at 1 s/step of scan range from 10° to 80°. The PVA hydrogel-based fabric composites were fixed into an entangled small ball and put in a sample holder to analyze the crystallographic peaks. The system contained art X'Celerator detector of the X'Pert Pro that allows for quick data collection. The analysis of XRD data is carried out by comparing the obtained peaks with the literature.

*2.2.5. Tensile Strength.* The tensile strength of the hydrogel composite was investigated per ISO 13934-2 standard. This standard is also known as the grab method to determine the maximum force that a sample can bear. A 200 mm × 100 mm specimen is gripped in the jaws and then extended at a constant rate until it ruptures. The force was then recorded at which the specimen got ruptured. The physical conditions for this test are $20 \pm 2°C$ temperature and $(65 \pm 2)\%$ relative humidity.

*2.2.6. Water Absorbency.* To investigate the fibers' water absorbency, the ASTM D570 standard was utilized. The samples were initially dried for 24 hours at 50°C in an oven and weighed on an analytical balance with a least count of 0.1 mg ($W_d$). Then, the preconditioned samples were immersed in distilled water at ambient temperature and pressure for 24 hours. After removing the samples, they were patted dry and reweighed ($W_w$). The water absorbency was calculated using equation (1) after determining the dry and wet weights of the fibers.

$$\text{Water absorption} \left(\frac{g}{g}\right) = \frac{W_w - W_d}{W_d} \times 100. \quad (1)$$

## 3. Result and Discussion

Microscopic images of all the samples were taken to investigate the surface morphology of the hydrogel composites. Figures 2(a), 2(d), and 2(g) show the neat/pure fabric surfaces of flax, polypropylene, and jute, respectively. These images show the neat fabrics showing the protruding fibers on the surface of the fabric and the free areas/spaces available in the woven fabric. Figures 2(b), 2(e), and 2(h) present the PVA yarn stitched on flax, polypropylene, and jute fabrics. These images show that flax, polypropylene, and jute fabric are successfully stitched with PVA yarn. The stitched PVA yarn can be seen in all these figures. The PVA hydrogel-based woven fabric composites from three different fabrics are shown in Figures 2(c), 2(f), and 2(i). These figures indicate that fibers are covered with PVA hydrogel, and the size of the free spaces is reduced due to the presence of the hydrogel. The PVA hydrogel layer is formed after simultaneously dissolving and crosslinking with borax and is present on the surface and in between the yarns in the woven fabric.

Figure 3 displays SEM images that reveal the surface characteristics of the hydrogel composite. Figure 3(a) exhibits a rough surface of flax-reinforced PVA hydrogel composite, which is attributed to the presence of PVA hydrogel. Figure 3(b) illustrates the impregnation of fibers with PVA hydrogel, surrounded by a plane matrix, while Figure 3(c) demonstrates the rough surface of jute-reinforced PVA hydrogel composite and the adhesion of fibers with each other through the PVA matrix. These images indicate that the PVA hydrogel contributes to the roughness of the surface and enhances the connectivity between fibers.

*3.1. FTIR Analysis.* FTIR analysis was performed to investigate the presence of hydrogel of PVA on different fabrics. FTIR spectra of all the fabric samples are given in Figure 4 which shows different peaks corresponding to the different functional groups. (A)–(C) in Figures 4(a) and 4(c) represent the FTIR spectra of flax-reinforced PVA hydrogel composite and jute-reinforced PVA hydrogel composite at different PVA volume fractions. All the samples show a broadening peak with a peak point around $3300 \, cm^{-1}$ which corresponds to the stretching of the -OH functional group [31]. The depth of the -OH peak increases to some extent by increasing the fiber volume ratio of PVA yarn. The possible reason is that all the -OH groups might not be completely crosslinked with borax. Except this, flax and jute are cellulosic fibers, so -OH groups of cellulose were not completely dissolved or crosslinked with the borax. The peak at $2924 \, cm^{-1}$ in the spectra of flax and jute composites corresponds to the -CH stretching [32, 33]. The peak around $1730 \, cm^{-1}$ corresponds to the C=O group. The peak around $1350 \, cm^{-1}$ corresponds to the primary -CH stretching. Another peak is seen around $1088 \, cm^{-1}$ which corresponds to the C-O group [34]. All these peaks confirm the structure of flax and jute fibers. Except for these peaks, there are two more peaks present in this structure at $1416 \, cm^{-1}$ and

$1325 \, cm^{-1}$ attributed to the $CH_2$ bending and CH wagging due to the presence of PVA hydrogel [35] onto the flax and jute fabrics. A very narrow peak can be seen around $650 \, cm^{-1}$ which could be due to the vibration of O-B-O bonds [32, 34]. All these peaks confirm the presence of PVA hydrogel on flax and jute fabrics.

(A)–(C) in Figure 4(b) show the FTIR spectra of polypropylene-reinforced PVA hydrogel composite at different PVA volume fractions. All these spectra show the same peaks with slightly different peak intensities due to the different volume fractions of PVA yarn. The peaks at $2950 \, cm^{-1}$ and $2920 \, cm^{-1}$ correspond to the asymmetric stretching of $CH_3$ and $CH_2$, respectively. Narrower peaks near $1450 \, cm^{-1}$ and $1380 \, cm^{-1}$ correspond to the bending of $CH_3$ [36]. The vibrational peaks at 840, 1000, and $1170 \, cm^{-1}$ are indicative of the characteristic vibrations associated with the presence of terminal unsaturated $CH_2$ groups in isotactic polypropylene [37]. A peak with slight intensity can be seen at around $3300 \, cm^{-1}$ which corresponds to the OH groups due to the presence of PVA on the surface of polypropylene fabric. Another peak at $1325 \, cm^{-1}$ corresponds to the CH wagging due to PVA. A very narrow peak can be seen around $650 \, cm^{-1}$ which could be due to the vibration of O-B-O bonds [32, 34].

*3.2. X-Ray Diffraction Analysis.* X-ray analysis was performed to investigate the crystalline peaks of pure fabrics and fabric-reinforced PVA composites. X-ray diffractogram of the three optimized composite samples (0.25% fiber volume fraction) was performed, and their results are given in Figure 5. Figure 5(a) shows the XRD peak of pure flax fabric showing the crystalline peaks at around 15° (101) and 22° (002) confirming cellulose 1 [38]. The same peaks can be observed in Figure 5(b) with an extra peak of PVA at 19° (110) confirming the presence of PVA hydrogel onto the flax fabric [39]. XRD spectra for pure jute fabric and jute-reinforced PVA composite are given in Figures 5(e) and 5(f), respectively. Both spectra show the peaks at approximately $2\theta = 16$ and 22° that arise from the cellulose (110), (200), and planes [40]. However, an extra peak at around 19° (110) can be seen for PVA hydrogel confirming the development of jute-reinforced PVA hydrogel composite. Figures 5(c) and 5(d) display distinct peaks centered at the $2\theta$ angles of 14°, 17°, and 19° for the polypropylene fabric, corresponding to the $\alpha$-form crystallographic planes (110), (040), and (130), respectively [41]. The peak of PVA might be merged with the polypropylene peak at 19° and cannot be seen as a separate peak. A low-intensity peak can be seen around 35° in all the composite samples in b, d, and f that corresponds to the excess of borax (024) which remains in the hydrogel composite and becomes crystallized after drying [42].

*3.3. Tensile Strength.* The tensile strength of the neat fabric and the hydrogel composite is given in Figure 6(a). It can be seen in Figure 6(a) that the tensile strength of the hydrogels is greater than that of their corresponding neat fabrics.
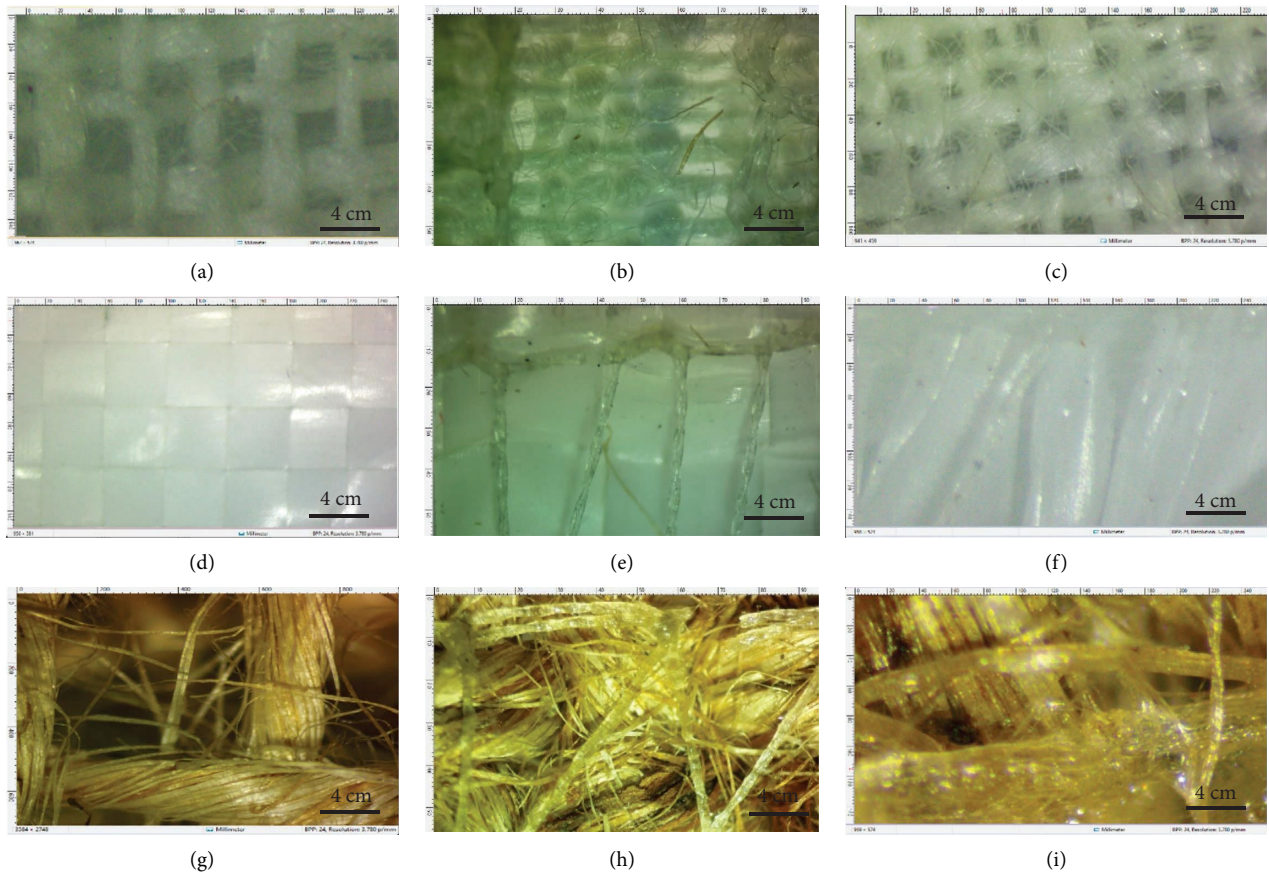
Figure 2: Microscopic images of neat fabrics ((a) flax, (d) polypropylene, and (g) jute), stitched fabrics ((b) flax, (e) polypropylene, and (h) jute), and fabric-reinforced PVA hydrogel composites ((c) flax, (f) polypropylene, and (i) jute).
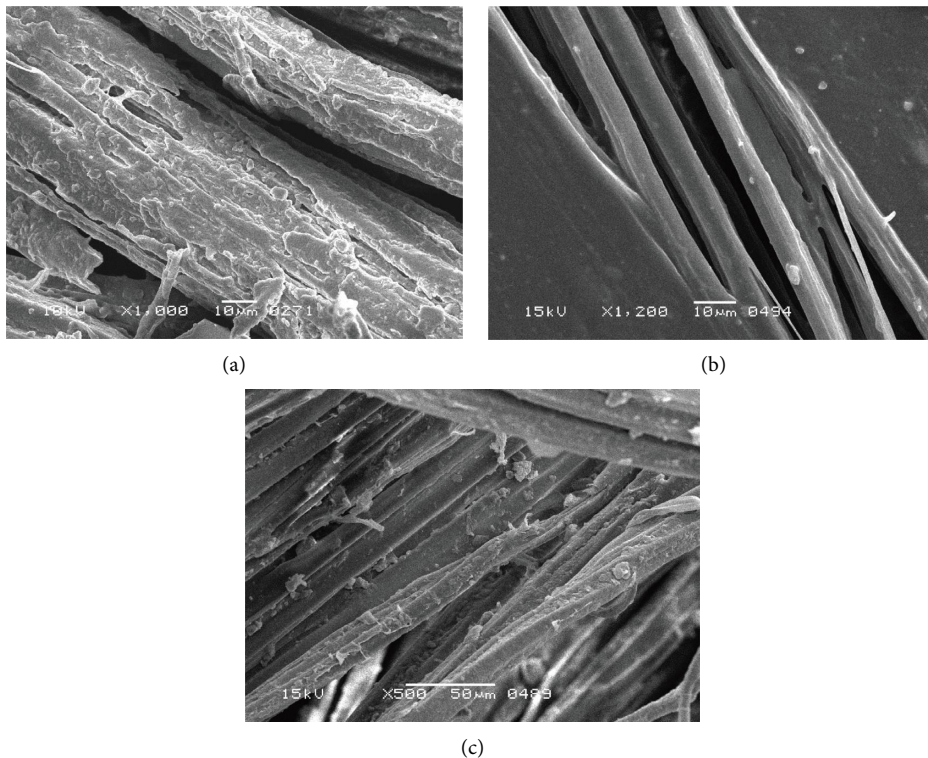


Figure 3: SEM images of fabric-reinforced PVA hydrogel composites: (a) flax, (b) polypropylene, and (c) jute.
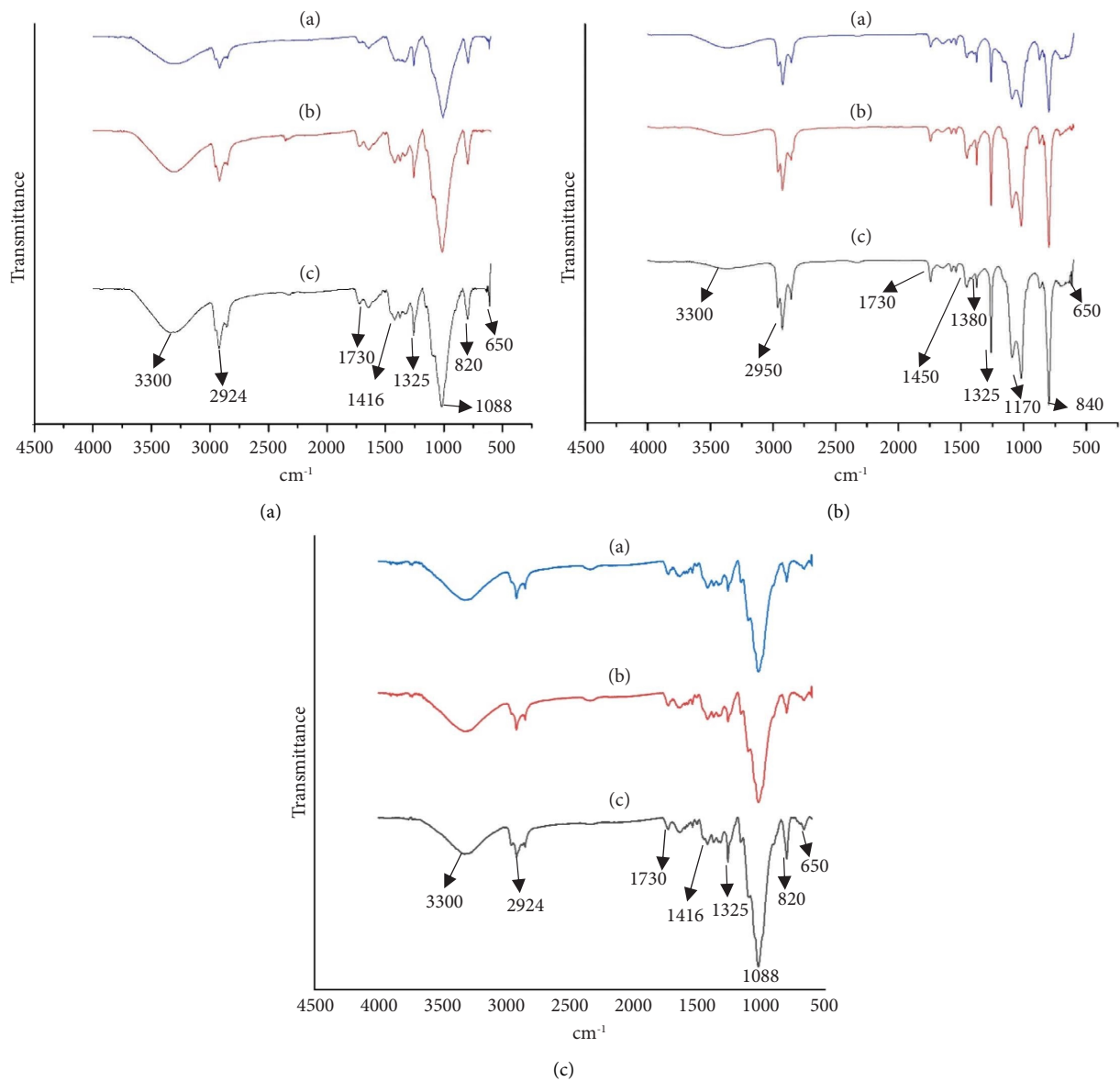
Figure 4: FTIR spectra of (a) flax-reinforced PVA composite with different fiber volume fractions: (A) 0.20; (B) 0.25; (C) 0.30; (b) polypropylene-reinforced hydrogel with different fiber volume fractions: (A) 0.20; (B) 0.25; (C) 0.30; and (c) jute-reinforced hydrogel with different fiber volume fractions: (A) 0.20; (B) 0.25; (C) 0.30.

Samples 1–3 represent the flax fabric-reinforced hydrogels with 0.20%, 0.25%, and 0.5% corresponding PVA yarns. The strength of the flax fabric-reinforced hydrogel composite is greater than that of the other two hydrogel composites. The tensile strength of the flax-based hydrogel increases with the increase in PVA yarn content. The possible reason is that more PVA yarn per unit area means more crosslinking of the PVA molecules with each other and with the flax fabric which ultimately increases the tensile strength of the fabric. Samples 4–6 represent the polypropylene fabric and hydrogel composite. It shows the same trend as in the case of flax fabric. The tensile strength of the hydrogel is more than that of their neat fabric because of crosslinking of PVA molecules. The same trend can be seen for the jute fabric as

well which is represented by samples 7–9. The increase in the strength of the jute-based hydrogel composite is more than that of the other two (flax and polypropylene) composites. The possible reason is that the PVA molecules of the hydrogel crosslinked with each other as well as with the molecules of the jute fabric resulting in more tensile strength of the composites. But the flax fabric-reinforced hydrogel composite showed the highest tensile strength among all the samples. From Figure 6(b), it can be seen from the stress-strain curve that by increasing the PVA percentage in the making of hydrogel composite, the structure becomes rigid. Elongation at break is greater for polypropylene hydrogel samples than the flax and jute-based hydrogel-reinforced samples. The reason is that polypropylene is a synthetic fiber
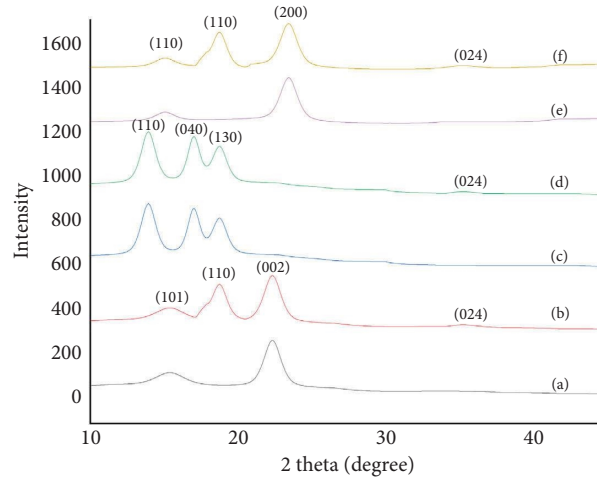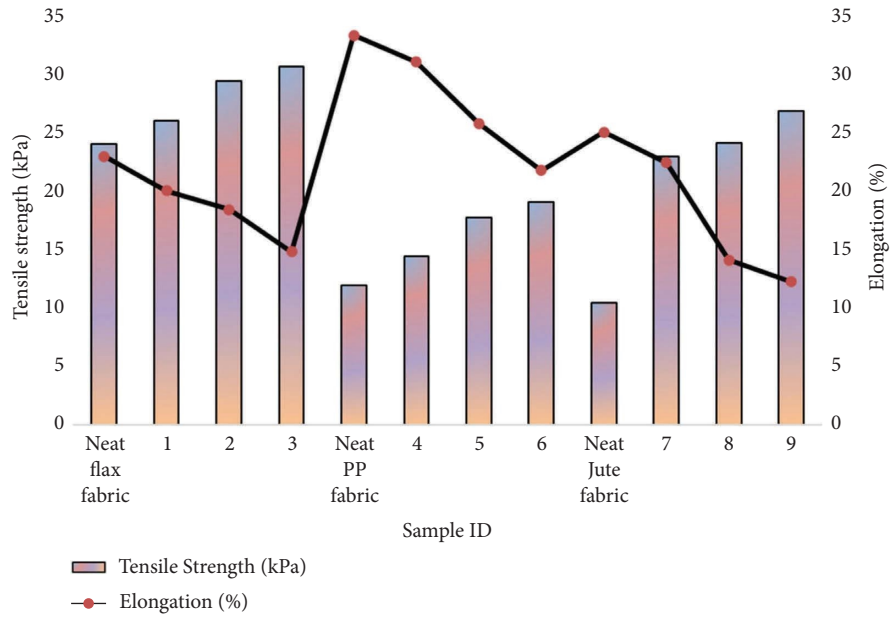
FIGURE 5: X-ray diffractogram of (a) pure flax fabric, (b) flax-reinforced PVA composite, (c) pure polypropylene fabric, (d) polypropylene-reinforced PVA composite, (e) pure jute fabric, and (f) jute-reinforced PVA composite.
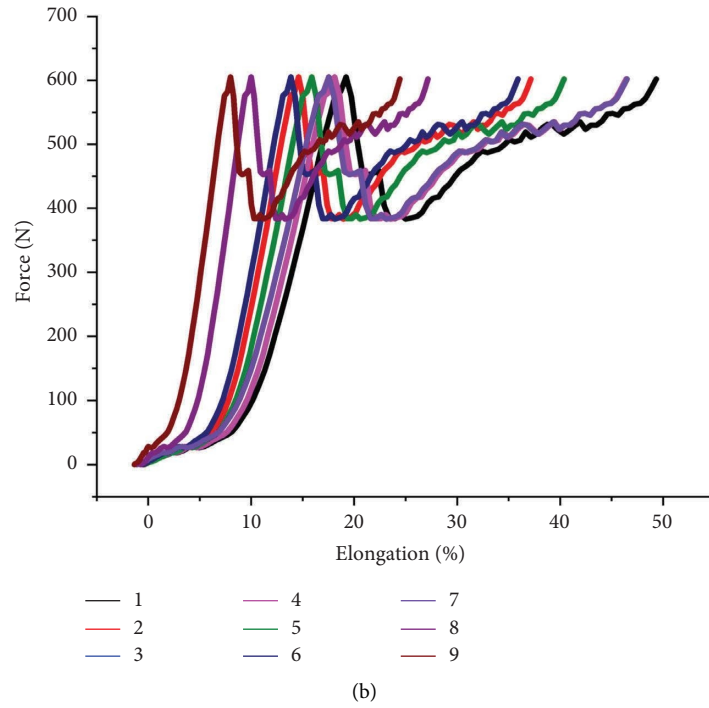


(a)

FIGURE 6: Continued.

(b)

FIGURE 6: (a) Breaking strength of pure fabrics and fabric-reinforced hydrogel composites. (b) Stress-strain curve of hydrogel composites.
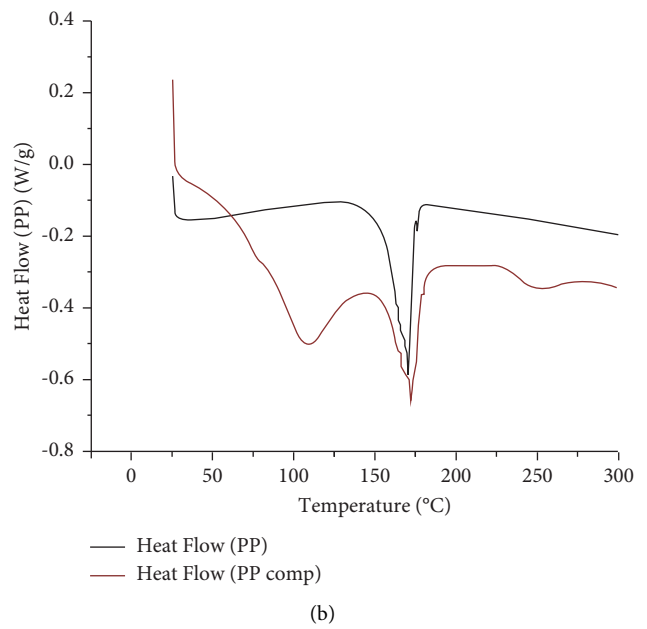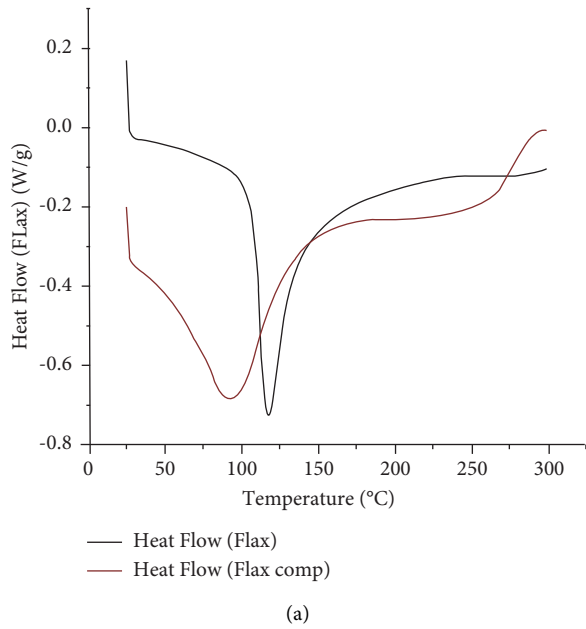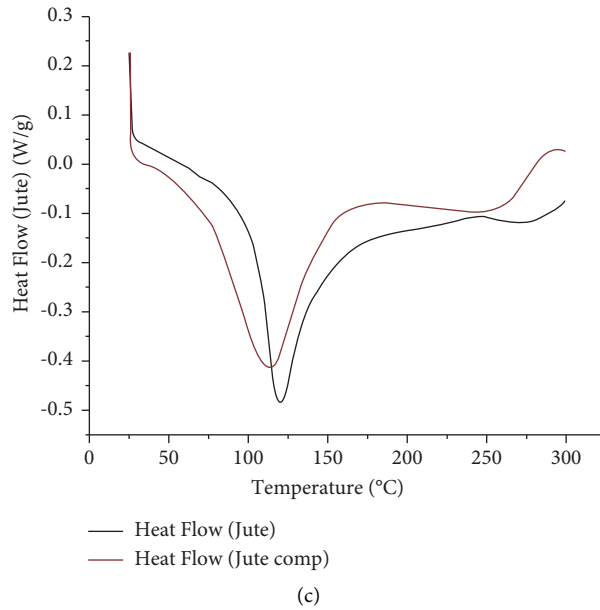


(a)



(b)

FIGURE 7: Continued.

(c)

FIGURE 7: DSC analysis of (a) neat flax fabric and flax-reinforced hydrogel composite, (b) neat PP fabric and PP-reinforced hydrogel composite, and (c) neat jute fabric and jute-reinforced hydrogel composite.
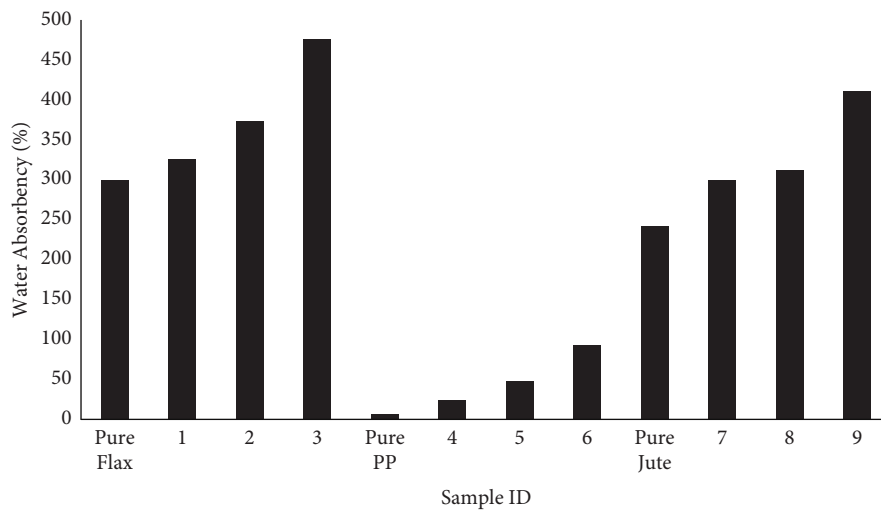


FIGURE 8: Water absorbency of pure fabrics and fabric-reinforced PVA composite hydrogels.

with soft points in its molecular structure which makes it stretch with the application of force, and hence it has more elongation at break than other samples.

3.4. Thermal Analysis. Thermal analysis of the neat fabrics and fabric-reinforced PVA hydrogel composites was performed using differential scanning calorimetry (DSC). Figure 7 shows the DSC analysis for the neat/pure fabrics of flax, polypropylene, and jute neat fabrics and their reinforced composites. The results in Figure 7 revealed that there is a change in the endothermic peaks for the pure fabrics and fabric-reinforced hydrogels. The endothermic peak of the pure flax (Figure 7(a)) and jute fabric (Figure 7(c)) is found

near 100°C, and the endothermic peak of the flax-reinforced hydrogel composite was found before 100°C which confirms the PVA deposition and crosslinking on the flax fabric because pure PVA hydrogel shows a broad endothermic peak around 100°C which is the melting temperature ($T_m$) of PVA hydrogels [43]. On the other hand, the change in the endothermic peak of jute fabric by incorporating the PVA confirms the formation of hydrogel composite. A sharp endothermic peak can be seen at 160°C in the case of neat polypropylene fabric which is the melting temperature ($T_m$) of polypropylene [44]. In the case of polypropylene-reinforced PVA composite, two endothermic peaks at 110°C ($T_m$ of PVA hydrogel) and 160°C ($T_m$ of polypropylene fabric) can be seen in Figure 7(b).

*3.5. Water Absorbency.* The water absorbency of pure fabrics and fabric-reinforced PVA composite hydrogels is given in Figure 8. For pure fabric, flax showed the maximum water absorbency value while polypropylene showed the least. The reason is that jute and flax are cellulosic materials that can absorb water due to the hydrogen bonding present between the cellulosic molecules and water molecules. Polypropylene is a hydrophobic polymer that does not have an affinity towards water molecules, and hence it showed the least value of water absorbency. The water absorbency of PVA hydrogel composites is greater than their respective pure fabrics. Since hydrogel has a strong capability of water absorption, composites have more water absorbency values than pure fabric. Flax-reinforced PVA hydrogel composites (samples 1–3) show the highest water absorbency property than other fabric-reinforced composites. Polypropylene (samples 4–6) shows the least water absorbency of the composite hydrogels. Since pure polypropylene shows the least water absorbency, the composite shows improved values of water absorbency due to PVA deposition on polypropylene. The effect of different PVA concentrations on the water absorbency of the PVA composite is given in Figure 8 which shows that the absorbency values increase with the increase in PVA concentration. The reason is that by increasing PVA concentration in composites, there will be more molecules present in the composite to attract the water molecules and hence increase the water absorbency.

## 4. Conclusion

Woven fabric-reinforced PVA hydrogel composite was successfully developed by treating PVA-stitched woven fabric with aqueous borax. The stitched PVA yarn was simultaneously dissolved and crosslinked by treating it in borax solution and became a hydrogel structure. The FTIR and X-ray diffraction analysis confirms the PVA hydrogel on the woven fabrics. Jute and polypropylene-reinforced PVA hydrogel composites are more thermally stable than flax-reinforced composites. The tensile strength results revealed that fabric-reinforced hydrogel composites have more strength than their corresponding neat fabrics. Flax-reinforced hydrogel composite shows the highest tensile strength (590 N) than jute (517 N) and polypropylene (367 N) composites. Tensile strength of all the fabric-reinforced samples increased by increasing the PVA yarn content in the composite structure. Polypropylene-reinforced PVA hydrogel composite showed the highest elongation percentage among all the samples because of its synthetic nature. Force-elongation curve shows that the rigidity of the composite structure increased by increasing the PVA yarn content in the structure. Water absorbency results have shown that hydrogel composites have more water absorption than their respective neat fabrics. Flax-reinforced hydrogel composite has the highest water absorbency (476%) while PP hydrogel composite showed the least water absorbency (93%). Hydrogel composites with high strength have the potential to be utilized as hygroscopic materials for erosion control and packaging [45].

## Data Availability

The data used to support the findings of this study are available from the corresponding author upon request.

## Conflicts of Interest

The authors declare that they have no conflicts of interest.

## References

[1] A. S. Hoffman, "Hydrogels for biomedical applications," *Advanced Drug Delivery Reviews*, vol. 64, pp. 18–23, 2012.

[2] Q. Chai, J. Yang, and X. Yu, "Hydrogels for biomedical applications: their characteristics and the mechanisms behind them," *Gels*, vol. 23, 2017.

[3] N. A. Peppas and A. G. Mikos, "Preparation methods and structure of hydrogels," *Hydrogels in Medicine and Pharmacy*, vol. 1, pp. 1–27, 1986.

[4] M. Radwan, O. Al-Sweasy, and H. Elazab, "Preparation of hydrogel based on acryl amide and investigation of different factors affecting rate and amount of absorbed water," *Agricultural Sciences*, vol. 08, no. 2, pp. 161–170, 2017.

[5] F. Ahmad, B. Mushtaq, F. A. Butt et al., "Synthesis and characterization of nonwoven cotton-reinforced cellulose hydrogel for wound dressings," *Polymers*, vol. 13, no. 23, p. 4098, 2021.

[6] N. Sahu, D. Gupta, and U. Nautiyal, "Hydrogel: preparation, characterization and applications," *Asian Pacific Journal of Nursing and Health Sciences*, vol. 3, no. 1, pp. 1–11, 2020.

[7] S. Ma, S. Wang, Q. Li, Y. Leng, L. Wang, and G. H. Hu, "A novel method for preparing poly(vinyl alcohol) hydrogels: preparation, characterization, and application," *Industrial & Engineering Chemistry Research*, vol. 56, no. 28, pp. 7971–7976, 2017.

[8] Z. Sun, C. Song, C. Wang, Y. Hu, and J. Wu, "Hydrogel-based controlled drug delivery for cancer treatment: a review," *Molecular Pharmaceutics*, vol. 17, no. 2, pp. 373–391, 2020.

[9] Y. Cai, J. Che, M. Yuan, X. Shi, W. Chen, and W. E. Yuan, "Effect of glycerol on sustained insulin release from PVA hydrogels and its application in diabetes therapy," *Experimental and Therapeutic Medicine*, vol. 12, no. 4, pp. 2039–2044, 2016.

[10] J. Li, F. Yu, G. Chen et al., "Moist-retaining, self-recoverable, bioadhesive, and transparent in situ forming hydrogels to accelerate wound healing," *ACS Applied Materials and Interfaces*, vol. 12, no. 2, pp. 2023–2038, 2020.

[11] L. Zhu, Y. Liu, Z. Jiang, E. Sakai, J. Qiu, and P. Zhu, "Highly temperature resistant cellulose nanofiber/polyvinyl alcohol hydrogel using aldehyde cellulose nanofiber as cross-linker," *Cellulose*, vol. 26, no. 9, pp. 5291–5303, 2019.

[12] S. Ma, M. Scaraggi, D. Wang et al., "Nanoporous substrate-infiltrated hydrogels: a bioinspired regenerable surface for high load bearing and tunable friction," *Advanced Functional Materials*, vol. 25, no. 47, pp. 7366–7374, 2015.

[13] P. Lin, R. Zhang, X. Wang et al., "Articular cartilage inspired bilayer tough hydrogel prepared by interfacial modulated polymerization showing excellent combination of high load-bearing and low friction performance," *ACS Macro Letters*, vol. 5, no. 11, pp. 1191–1195, 2016.

[14] Z. Wang, F. Tao, and Q. Pan, "A self-healable polyvinyl alcohol-based hydrogel electrolyte for smart electrochemical

capacitors," *Journal of Materials Chemistry*, vol. 4, no. 45, pp. 17732–17739, 2016.

[15] Y. Li, C. Hu, J. Lan et al., "Hydrogel-based temperature sensor with water retention, frost resistance and remoldability," *Polymer*, vol. 186, Article ID 122027, 2020.

[16] B. K. Tan, Y. Ching, S. C. Poh, L. C. Abdullah, and S. N. Gan, "A review of natural fiber reinforced poly(vinyl alcohol) based composites: application and opportunity," *Polymers*, vol. 7, no. 11, pp. 2205–2222, 2015.

[17] F. Ahmad, K. Shehzad Akhtar, W. Anam et al., "Recent developments in materials and manufacturing techniques used for sports textiles." edited by hossein roghanimamaqani," *International Journal of Polymer Science*, vol. 2023, Article ID 2021622, 2023.

[18] F. Azam, F. Ahmad, S. Ahmad, M. S. Zafar, and Z. Ulker, "Preparation and Characterization of Alginate Hydrogel Fibers Reinforced by Cotton for Biomedical Applications," *Polymers*, vol. 34, 2022.

[19] F. Azam, F. Ahmad, Z. Uddin et al., "A review of the fabrication methods, testing, and performance of face masks," *International Journal of Polymer Science*, vol. 2022, Article ID 2161869, 20 pages, 2022.

[20] F. Azam and S. Ahmad, "Fibers for agro textiles BT - fibers for technical textiles," in *Sheraz Ahmad, Abher Rasheed, and Yasir Nawab,*Springer International Publishing, Berlin, Germany, 2020.

[21] D. Zhang, J. Duan, D. Wang, and S. Ge, "Effect of preparation methods on mechanical properties of PVA/HA composite hydrogel," *Journal of Bionics Engineering*, vol. 7, no. 3, pp. 235–243, 2010.

[22] J. A. Stammen, S. Williams, D. N. Ku, and R. E. Guldberg, "Mechanical properties of a novel PVA hydrogel in shear and unconfined compression," *Biomaterials*, vol. 22, no. 8, pp. 799–806, 2001.

[23] Y. Chen, J. Li, J. Lu, M. Ding, and Y. Chen, "Synthesis and properties of poly(vinyl alcohol) hydrogels with high strength and toughness," *Polymer Testing*, vol. 108, Article ID 107516, 2022.

[24] F. Azam, F. Ahmad, Z. Ulker et al., "The role and applications of aerogels in textiles," *Advances in Materials Science and Engineering*, vol. 2022, Article ID 2407769, 22 pages, 2022.

[25] Y. Huang, D. R. King, T. L. Sun et al., "Energy-dissipative matrices enable synergistic toughening in fiber reinforced soft composites," *Advanced Functional Materials*, vol. 27, no. 9, Article ID 1605350, 2017.

[26] M. Arjmandi, M. Ramezani, T. Bolle, G. Köppe, T. Gries, and T. Neitzert, "Mechanical and tribological properties of a novel hydrogel composite reinforced by three-dimensional woven textiles as a functional synthetic cartilage," *Composites Part A: Applied Science and Manufacturing*, vol. 115, pp. 123–133, 2018.

[27] J. L. Holloway, A. M. Lowman, M. R. VanLandingham, and G. R. Palmese, "Interfacial optimization of fiber-reinforced hydrogel composites for soft fibrous tissue applications," *Acta Biomaterialia*, vol. 10, no. 8, pp. 3581–3589, 2014.

[28] F. Ahmad, B. Mushtaq, F. A. Butt, A. Rasheed, and S. Ahmad, "Preparation and characterization of wool fiber reinforced nonwoven alginate hydrogel for wound dressing," *Cellulose*, vol. 28, no. 12, pp. 7941–7951, 2021.

[29] M. Trad, W. Miled, S. Benltoufa et al., "Chitosan hydrogel-coated cotton fabric: antibacterial, PH-responsiveness, and physical properties," *Journal of Applied Polymer Science*, vol. 135, no. 34, p. 46645, 2018.

[30] U. Koc, Y. Aykut, and R. Eren, "Natural fibers woven fabric reinforced hydrogel composites for enhanced mechanical properties," *Journal of Industrial Textiles*, vol. 51, no. 4, pp. 6315S–6332S, 2020.

[31] M. Lim, H. Kwon, D. Kim, J. Seo, H. Han, and S. B. Khan, "Highly-enhanced water resistant and oxygen barrier properties of cross-linked poly(vinyl alcohol) hybrid films for packaging applications," *Progress in Organic Coatings*, vol. 85, pp. 68–75, 2015.

[32] S. Spoljaric, A. Salminen, N. D. Luong, and J. Seppälä, "Stable, self-healing hydrogels from nanofibrillated cellulose, poly(-vinyl alcohol) and borax via reversible crosslinking," *European Polymer Journal*, vol. 56, pp. 105–117, 2014.

[33] R. Rudra, V. Kumar, and P. P. Kundu, "Acid catalysed cross-linking of poly vinyl alcohol (PVA) by glutaraldehyde: effect of crosslink density on the characteristics of PVA membranes used in single chambered microbial fuel cells," *RSC Advances*, vol. 5, no. 101, pp. 83436–83447, 2015.

[34] J. Han, Y. Yue, Q. Wu et al., "Effects of nanocellulose on the structure and properties of poly(vinyl alcohol)-borax hybrid foams," *Cellulose*, vol. 24, no. 10, pp. 4433–4448, 2017.

[35] I. M. Jipa, A. Stoica, M. Stroescu et al., "Potassium sorbate release from poly(vinyl alcohol)-bacterial cellulose films," *Chemical Papers*, vol. 66, no. 2, pp. 138–143, 2012.

[36] J. Fang, L. Zhang, D. Sutton, X. Wang, and T. Lin, "Needleless melt-electrospinning of polypropylene nanofibres," *Journal of Nanomaterials*, vol. 2012, Article ID 382639, 9 pages, 2012.

[37] V. Krylova and N. Dukštienė, "Synthesis and cS layers formed on polypropylene," *Journal of Chemistry*, vol. 2013, Article ID 987879, 11 pages, 2013.

[38] L. I. Mikhalovska, V. M. Gun'ko, A. A. Rugal et al., "Cottonised flax fibres vs. Cotton fibres: structural, textural and adsorption characteristics," *RSC Advances*, vol. 2, no. 5, pp. 2032–2042, 2012.

[39] V. Abhilash, N. Rajender, and K. Suresh, "Chapter 14 - X-ray diffraction spectroscopy of polymer nanocomposites," in *Didier Rouxel, and Deepalekshmi B T - Spectroscopy of Polymer Nanocomposites Ponnamma*, S. Thomas, Ed., vol. 410, William Andrew Publishing, Norwich, NY, USA, 2016.

[40] C. A. Correia, L. Mota De Oliveira, and T. Sanches Valera, "The influence of bleached jute fiber filler on the properties of vulcanized natural rubber," *Materials Research*, vol. 20, pp. 472–478, 2017.

[41] S. Wang, A. Ajji, S. Guo, and C. Xiong, "Preparation of microporous polypropylene/titanium dioxide composite membranes with enhanced electrolyte uptake capability via melt extruding and stretching," *Polymers*, vol. 9, no. 12, p. 110, 2017.

[42] R. I. Baron, M. Bercea, M. Avadanei, G. Lisa, G. Biliuta, and S. Coseri, "Green route for the fabrication of self-healable hydrogels based on tricarboxy cellulose and poly(vinyl alcohol)," *International Journal of Biological Macromolecules*, vol. 123, pp. 744–751, 2019.

[43] M. Zulfiqar, S. Y. Lee, A. A. Mafize, N. A. M. A. Kahar, K. Johari, and N. E. Rabat, "Efficient removal of Pb(II) from aqueous solutions by using oil palm bio-waste/MWCNTs

reinforced PVA hydrogel composites: kinetic, isotherm and thermodynamic modeling," *Polymers*, vol. 12, no. 2, p. 430, 2020.

[44] M. Jaziri, N. Barhoumi, V. Massardier, and F. Mélis, "Blending PP with PA6 industrial wastes: effect of the composition and the compatibilization," *Journal of Applied Polymer Science*, vol. 107, no. 6, pp. 3451–3458, 2008.

[45] U. Koc, Y. Aykut, and R. Eren, "One-step preparation of woven fabric-reinforced hydrogel composite," *Journal of Industrial Textiles*, vol. 50, no. 7, pp. 990–1005, 2019.